



## Ammonia sensor based on NASICON and Cr<sub>2</sub>O<sub>3</sub> electrode

Xishuang Liang, Tiegang Zhong, Hesong Guan, Fengmin Liu, Geyu Lu, Baofu Quan\*

State Key Laboratory on Integrated Optoelectronics Jilin University Region, College of Electronic Science and Engineering, Jilin University, Changchun 130012, PR China

### ARTICLE INFO

#### Article history:

Received 4 August 2008

Received in revised form 6 November 2008

Accepted 23 November 2008

Available online 3 December 2008

#### Keywords:

NH<sub>3</sub>

NASICON

Cr<sub>2</sub>O<sub>3</sub>

Gas sensor

### ABSTRACT

A compact tubular sensor based on NASICON (sodium super ionic conductor) and porous Cr<sub>2</sub>O<sub>3</sub> sensing electrode was designed for the detection of ammonia. The sensor gave excellent sensing properties to 50–500 ppm ammonia in air at 250–450 °C. The EMF value of the sensor was almost proportional to the logarithm of ammonia concentration, the sensitivity (slope) was –89 mV/decade at 350 °C. It was also seen that the sensor showed a good selectivity to ammonia, and an excellent resistance to water vapor. The sensor had speedy response kinetics to ammonia, the 90% response time to 50 ppm ammonia was 30 s, and the recovery time was 60 s.

© 2008 Elsevier B.V. All rights reserved.

### 1. Introduction

Ammonia is produced and utilized extensively in many chemical industries, fertilizer factories, refrigeration systems, food processing, medical diagnosis, fire power plants, etc. A leak in the system can result the health hazards [1]. Hence, the development of ammonia sensors is very important for the detection of ammonia. At present, some types of ammonia sensors, e.g., conductive type using metal oxide [1–4], organic thin film type [5,6] and optical fiber sensor [7], have been proposed. The solid electrolyte type sensors have been investigated for detecting CO<sub>2</sub>, H<sub>2</sub>S and SO<sub>2</sub> due to their highly selectivity, rapid and reproducible response [8–10]. But this type of sensors has been few studied for the ammonia gas sensor.

NASICON is one of the most important solid electrolyte materials and Cr<sub>2</sub>O<sub>3</sub> has been used for the ammonia or nitrogen oxide-sensitive material in some references [1]. In the present work, we tried to construct a compact solid electrolyte ammonia sensor by combining NASICON prepared by sol–gel process with porous Cr<sub>2</sub>O<sub>3</sub> electrode. The sensing mechanism was also suggested by investigating the catalytic behavior of ammonia on porous Cr<sub>2</sub>O<sub>3</sub>.

### 2. Experimental

#### 2.1. Synthesis of NASICON and analysis of Cr<sub>2</sub>O<sub>3</sub>

The NASICON precursor was prepared from ZrO(NO<sub>3</sub>)<sub>2</sub>, NaNO<sub>3</sub>, (NH<sub>4</sub>)<sub>2</sub>HPO<sub>4</sub> and Si(C<sub>2</sub>H<sub>5</sub>O)<sub>4</sub> by sol–gel process [8,9]. The porous Cr<sub>2</sub>O<sub>3</sub> sensing material was obtained by mixing multiple car-

bon nanotubes (Shenzhen Billnt Corporation, China, 10–30 nm for diameter) with Cr<sub>2</sub>O<sub>3</sub>, full grinded in the agate bowl and sintered at high temperatures. The adulteration proportion for carbon nanotubes was 10 wt%. The structure of NASICON was identified by X-ray diffraction (a Rigaku wide-angle X-ray diffraction D/max rA, using Cu K $\alpha$  radiation at wavelength  $\lambda = 0.1541$  nm) analysis. The surface morphology of NASICON and sensing electrode was identified by the scanning electron microscope (SEM) (JEOL JSM-7500F Field Emission Scanning Electron Microscope). To investigate the sensing mechanism of the NH<sub>3</sub> sensor, XPS (VG ESCA LAB MK II, Mg K $\alpha$ , 10<sup>-7</sup> Pa) was utilized to analyze the adsorbed species on the surface of porous Cr<sub>2</sub>O<sub>3</sub> after exposing to 2000 ppm ammonia at 350 °C for 10 h.

#### 2.2. Fabrication of the sensor

A sensor device was fabricated by using an alumina tube of 6 mm long, 0.8 and 1.2 mm in inner and outer diameter, respectively [8,9], as shown in Fig. 1. A thick film of NASICON was formed on the outer surface of the alumina tube by dipping NASICON precursor paste prepared by sol–gel process many times and sintering at 900 °C for 6 h. A couple of Au electrodes with mesh-shape were made on the two ends of the thick film of NASICON. For forming the sensing electrode of the ammonia sensor, porous Cr<sub>2</sub>O<sub>3</sub> paste was applied on an Au electrode, followed by sintering at 600 °C for 3 h. Finally, a Ni–Cr coil was set in the inner of the alumina tube as a heater.

#### 2.3. Measurement of sensing properties

Gas sensing properties of the sensor were measured by a conventional static mounting method. The sample gases containing different concentrations of NH<sub>3</sub>, CO, NO, CH<sub>4</sub> and H<sub>2</sub>, C<sub>7</sub>H<sub>8</sub> and

\* Corresponding author. Tel.: +86 43185168384; fax: +86 43185168417.  
E-mail address: [quanbf@mail.jlu.edu.cn](mailto:quanbf@mail.jlu.edu.cn) (B. Quan).

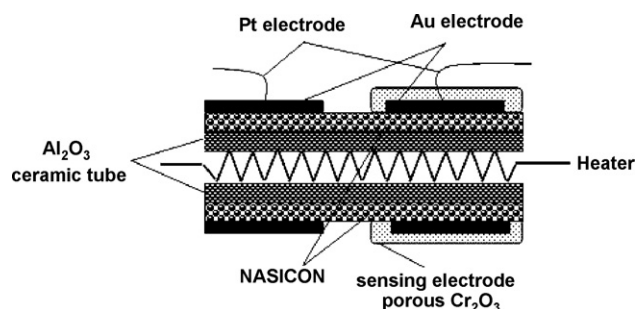


Fig. 1. Structure of NASICON-based electrochemical device attached with a layer of porous  $\text{Cr}_2\text{O}_3$  (electrode).

HCHO were obtained by diluting pure gases with  $\text{O}_2$  (21%) and  $\text{N}_2$  (79%). The electromotive force (EMF) was measured with a digital electrometer (Advanced, TR 8652) connected with a registering computer.

### 3. Results and discussion

#### 3.1. XRD and SEM analysis of NASICON

XRD analysis was used to confirm the phase compositions of NASICON and measure the mean crystallite size of NASICON, as shown in Fig. 2. From Fig. 2, NASICON was confirmed to have single phase of rhombohedral (JCPDS: 33-1314). In addition, the mean grain size of NASICON calculated with Debye–Scherrer equation was about 20 nm. SEM image of the NASICON surface shown in Fig. 3 exhibited that the crystallite size of NASICON was distributed in uniformly and the surface was comparatively compact.

#### 3.2. Sensing properties of the ammonia gas sensor

In this paper, the influence of C doping of the sensing electrode on the characteristics of the sensor was studied firstly. The contrast between the sensor based on the pure  $\text{Cr}_2\text{O}_3$  and 10 wt% C-doped  $\text{Cr}_2\text{O}_3$  was studied. Fig. 4 shows that, both the sensors based on pure  $\text{Cr}_2\text{O}_3$  and 10 wt% C-doped  $\text{Cr}_2\text{O}_3$  exhibited well characteristics to ammonia at 350 °C. Whereas the 10 wt% C-doped  $\text{Cr}_2\text{O}_3$  sensor showed much high sensitivity (−89 mV/decade) than the pure  $\text{Cr}_2\text{O}_3$ -based sensor (−57 mV/decade). From Fig. 5, it was seen that a lot of apertures appeared on the surface of the 10 wt% C-doped

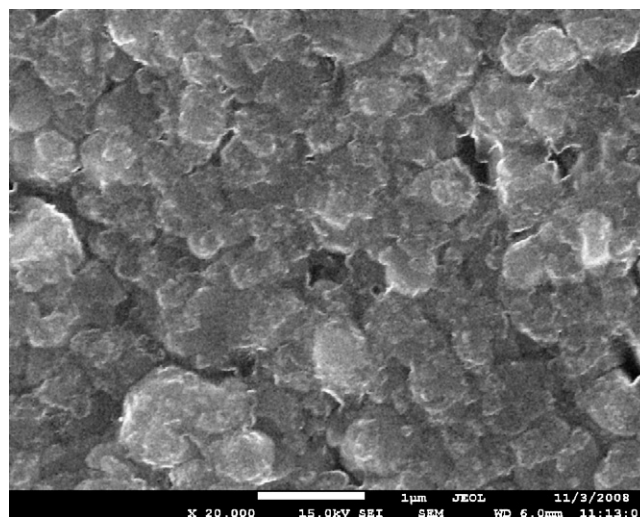


Fig. 3. The SEM image of the NASICON surface.

$\text{Cr}_2\text{O}_3$ , this could arise from that the carbon reacted with the oxygen in the air when the sensing electrode was doped with carbon, and came into being the porous  $\text{Cr}_2\text{O}_3$ . Therefore, the adsorption and diffusion of ammonia through the porous  $\text{Cr}_2\text{O}_3$  electrode were much facile than that through the pure  $\text{Cr}_2\text{O}_3$ . This could increase the amount of the ammonia molecule that participated in the chemical reaction. So that the carbon doping in the sensing electrode increased the sensitivity of the sensor to ammonia.

The sensitivity of the sensor depended on the operation temperatures, too. Fig. 6 shows that the EMF of the device attached with porous  $\text{Cr}_2\text{O}_3$  is perfectly linear to the logarithm of ammonia concentration, and the slopes were −58, −93, −89, −44 and −42 mV/decade at 250, 300, 350, 400, and 450 °C, respectively. With increasing the operating temperature, the slope tended to become large below 300 °C. At 300 °C, the largest value of the slopes occurred, but above 300 °C the slope tended to become small. This could arise from the amount of the ammonia molecular diffused through the porous  $\text{Cr}_2\text{O}_3$  electrode to the interface of NASICON and porous  $\text{Cr}_2\text{O}_3$  and adsorbed at the three terms interface of air, porous  $\text{Cr}_2\text{O}_3$  and NASICON increased along with the gradually increased operating temperature at low temperatures (<300 °C). In

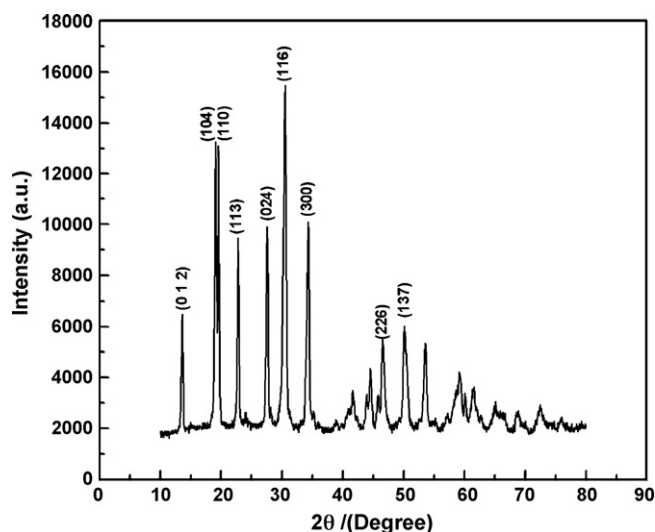


Fig. 2. XRD pattern of NASICON.

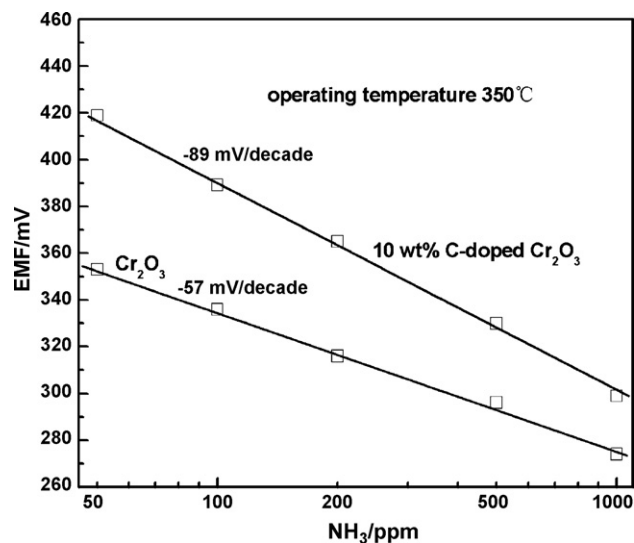


Fig. 4.  $\text{NH}_3$  sensing properties of sensor attached with the undoped  $\text{Cr}_2\text{O}_3$  and the 10 wt% C-doped  $\text{Cr}_2\text{O}_3$ .

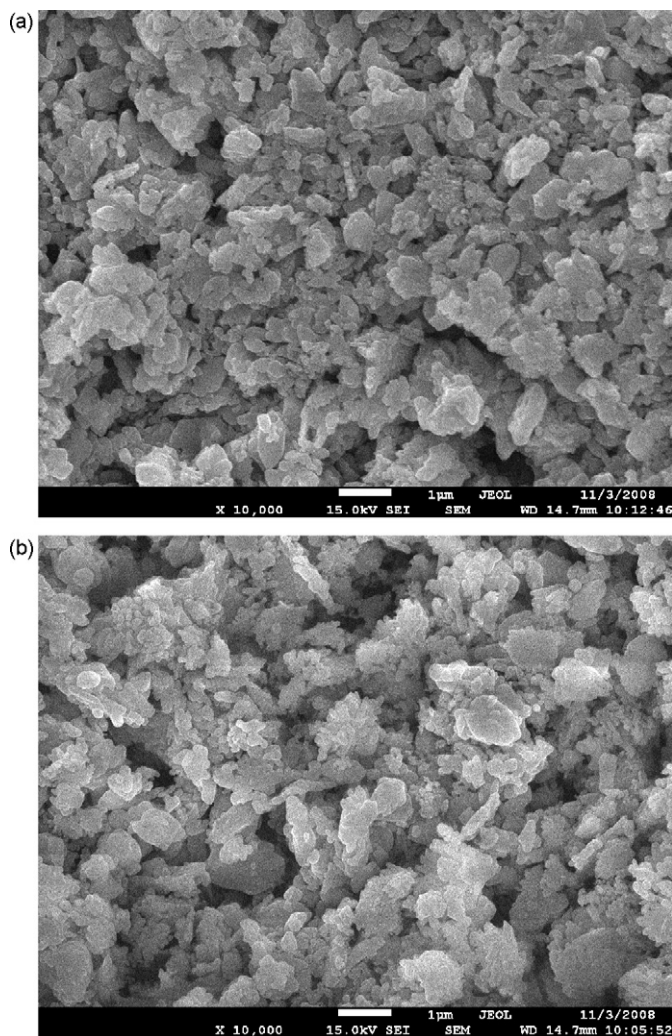


Fig. 5. The SEM images of (a) the undoped  $\text{Cr}_2\text{O}_3$  and (b) the 10 wt% C-doped  $\text{Cr}_2\text{O}_3$ .

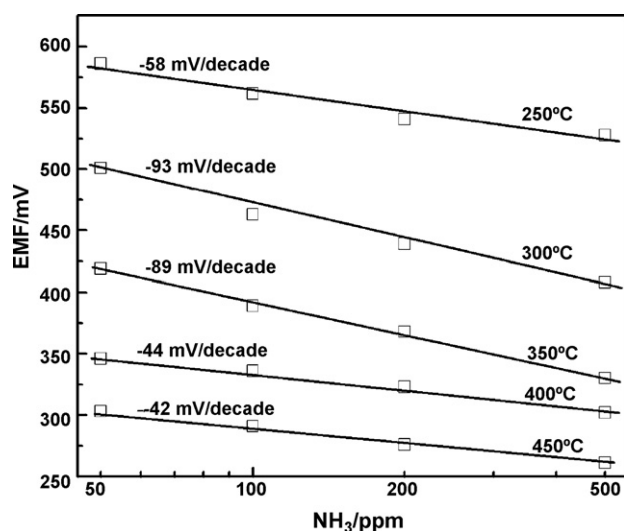


Fig. 6.  $\text{NH}_3$  sensing properties of the device attached with porous  $\text{Cr}_2\text{O}_3$  at different operating temperatures.

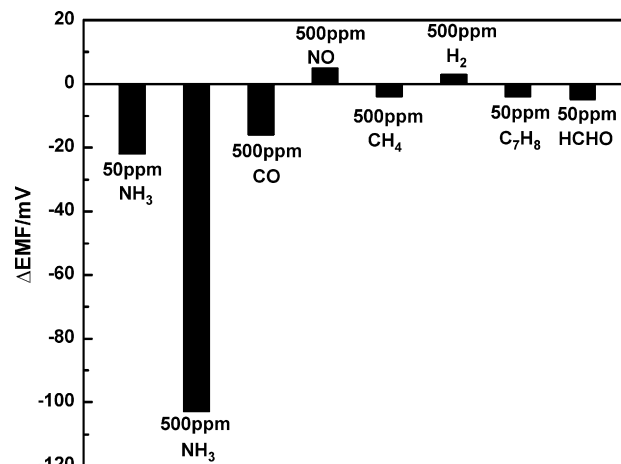
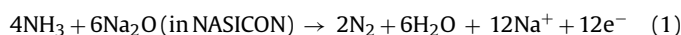


Fig. 7. Sensitivities of the device attached with porous  $\text{Cr}_2\text{O}_3$  to various gases at  $350^\circ\text{C}$ .

addition, a couple of electrochemical reactions (1) and (2) happen at the sensing electrode simultaneously, the chemical reactions at the three terms interface described by reactions (1) and (2) could be affected by the operating temperatures.



The occurring of the chemical reaction needed definite activated energy. At low temperatures ( $<300^\circ\text{C}$ ), it did not reach the activated energy, so that the  $\Delta\text{EMF}$  and the sensitivity of the sensor to ammonia increased along with the increased temperature. But above  $300^\circ\text{C}$ , the desorption of ammonia molecular exhibited more significant and the amount of ammonia molecule that adsorbed on the sensing electrode became less and less along with the increasing temperature. Just this result weakened the reactions (1) and (2). Hence the sensitivity of the sensor to ammonia decreased with the further increased operating temperature. However there were no distinction for the sensitivities of the sensor when operated at  $300$  and  $350^\circ\text{C}$ . From the perspective of selectivity,  $350^\circ\text{C}$  was selected for the operating temperature.

The cross-sensitivities of the device attached with porous  $\text{Cr}_2\text{O}_3$  to other various gases, i.e.  $\text{CO}$ ,  $\text{NO}$ ,  $\text{CH}_4$ ,  $\text{H}_2$ ,  $\text{C}_7\text{H}_8$  and  $\text{HCHO}$  were measured at  $350^\circ\text{C}$ , and the results obtained are shown in Fig. 7. The cross-sensitivities were rather small or almost none, indicating its excellent ammonia selectivity.

We also tested the effect of water vapor on the EMF value of sensor at  $350^\circ\text{C}$ , as shown in Fig. 8. There were large changes for the EMF value of the sensor at the humidity range of  $0\text{RH}\%$ – $20\text{RH}\%$ . And it changed small at the range of  $20\text{RH}\%$ – $75\text{RH}\%$ . Whereas it changed largely at high water humidity ( $>75\text{RH}\%$ ). This might be due to that there was water came into being in reaction (1) above. The existence of water could affect the process of reaction (1) and thereby the changes of the EMF value for the sensor at lower water humidity ( $<20\text{RH}\%$ ). At the range of  $20\text{RH}\%$ – $75\text{RH}\%$ , the effect of water on the EMF value was less because of the weak adsorption of water on the sensing electrode (porous  $\text{Cr}_2\text{O}_3$ ). However, at higher humidity ( $>75\text{RH}\%$ ), the influence of water on reaction (1) was strengthened further which led to the large changes of EMF value. And the specific relations between the humidity and EMF value of the sensor was very complicated and would be investigated in the future study.

The device attached with porous  $\text{Cr}_2\text{O}_3$  gave speedy response kinetics to dilute ammonia. Fig. 9 showed the response and recovery transients to various concentrations of ammonia at  $350^\circ\text{C}$ , and the 90% response time to 50 ppm and 500 ppm  $\text{NH}_3$  was 35 and 30 s, respectively, and the recovery time was 60 and 65 s, respectively.



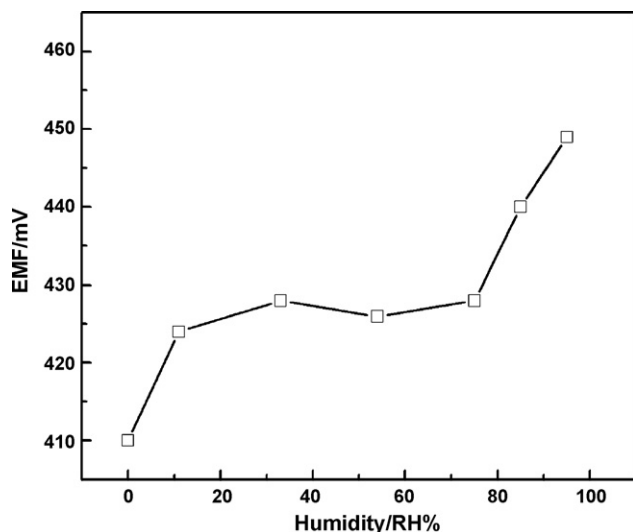


Fig. 8. The effect of water vapor on the EMF value of sensor at 350 °C.

### 3.3. Sensing mechanism of the $\text{NH}_3$ sensor

For explaining the sensing behavior of the device, XPS was applied for measuring the chemical shift of the related elements (e.g., O1s, Cr2p and N1s) on the surface of porous  $\text{Cr}_2\text{O}_3$  before (sample 1) and after (sample 2) exposure to 2000 ppm  $\text{NH}_3$  at 350 °C, the basic pressure of the XPS chamber was better than  $1 \times 10^{-7}$  Pa, as shown in Fig. 10. As a result, it was found that the chemical binding energies of O1s, and Cr2p did not change before and after exposure to 2000 ppm  $\text{NH}_3$ . There is no N element in sensing electrode after chemical reaction. This shows that  $\text{NH}_3$  comes into being gas status after reacting with sensing electrode. The resultants might be  $\text{N}_2$ ,  $\text{N}_2\text{O}$ , NO or  $\text{NO}_2$  and the most possible resultant is  $\text{N}_2$  according to the activated energy.

As described, the sensor using NASICON and porous  $\text{Cr}_2\text{O}_3$  electrode gave a good linear relationship between EMF and the logarithm of the concentration of ammonia as switching on dilute ammonia. Lu, Miura and Yamazoe have established a sensing mechanism involving mixed potentials for a group of sensors combining stabilized zirconia with oxide electrodes, such as  $\text{NO}_x$ ,  $\text{H}_2$ , CO sensors [11–13]. Therefore, a similar sensing mechanism would be attempted to apply for the present sensors.

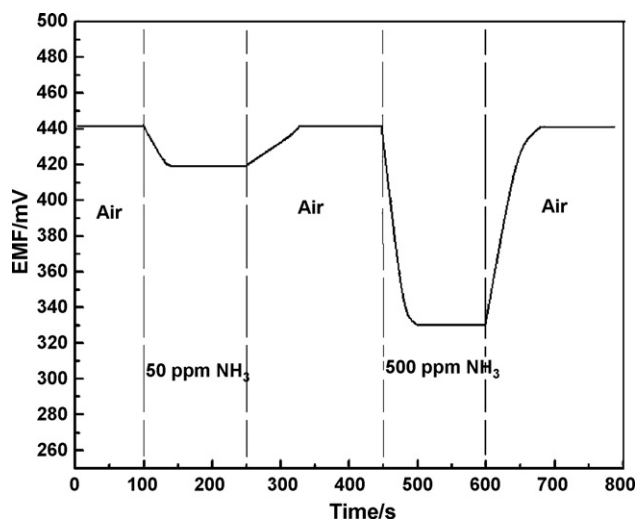


Fig. 9. Transient response and recovery characteristic when taking a switching change from air to different concentrations of ammonia.

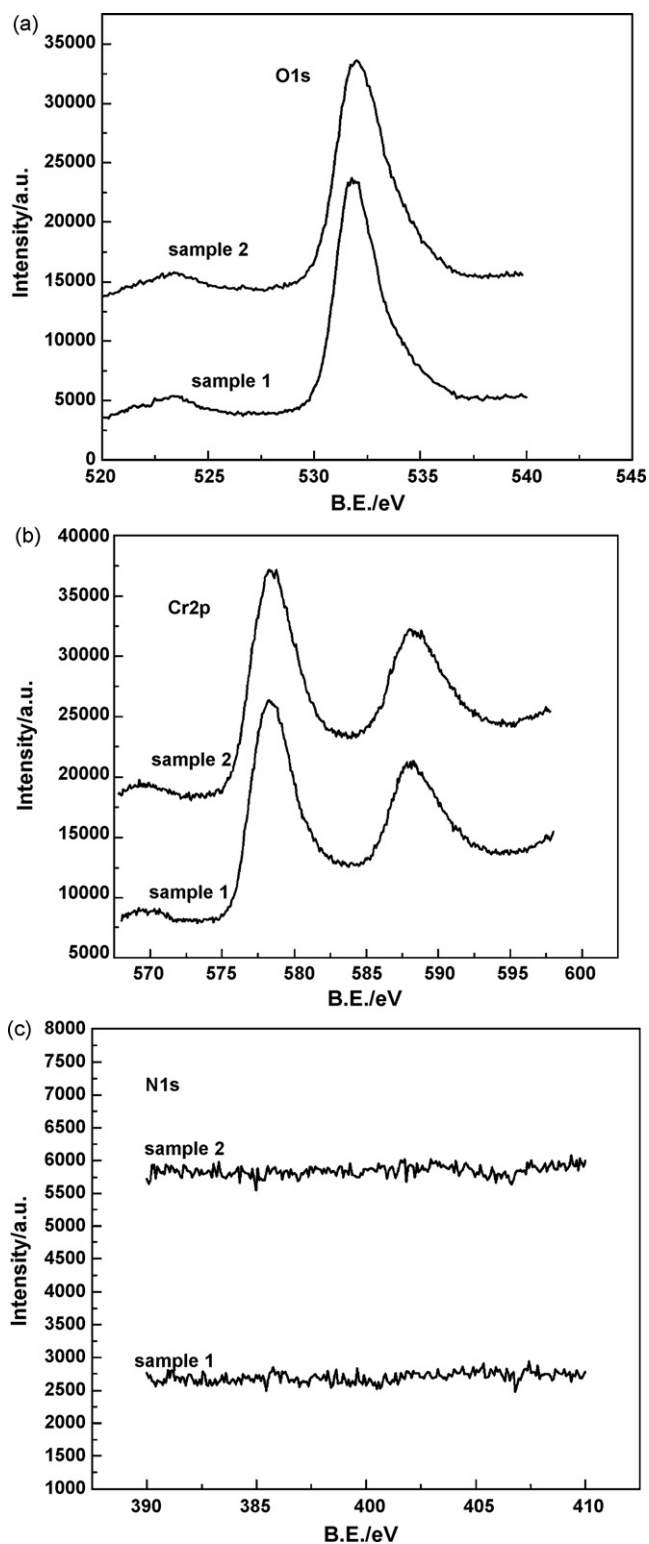


Fig. 10. XPS spectra of porous  $\text{Cr}_2\text{O}_3$  before (sample 1) and after (sample 2) exposure to 2000 ppm  $\text{NH}_3$  at 350 °C.

The sensor could be expressed with the following electrochemical cell:



We consider that a couple of electrochemical reactions (1) and (2) above happen at the sensing electrode simultaneously.

These two electrochemical reactions construct a local cell at the sensing electrode, and when the rates of the reactions were equal to each other, they arrive at a dynamic equilibrium, and the electrode potential at the sensing electrode was the mixed potential [12]. By treating Eqs. (1) and (2) with the same process described in [11–13], we could obtain the following equation.

$$E_M = E_0 + nA \ln C_{O_2} - mA \ln C_{NH_3} \quad (4)$$

Here

$$E_0 = \frac{RT}{2(3\alpha_1 + 2\alpha_2)F} \ln \frac{B_2}{B_1} + \frac{3\alpha_1 E_{NH_3}^0 + 2\alpha_2 E_{O_2}^0}{3\alpha_1 + 2\alpha_2}$$

$$A = \frac{RT}{2(3\alpha_1 + 2\alpha_2)F}$$

Here  $C_{O_2}$  and  $C_{NH_3}$  are the concentrations of  $O_2$  and  $NH_3$ , and  $B_1$ ,  $B_2$ ,  $m$  and  $n$  are the constants,  $F$  the Faraday constant,  $R$  the gas constant and  $T$  the absolute temperature,  $E_{NH_3}^0$  and  $E_{O_2}^0$  represent electrode potential at equilibrium,  $\alpha$  represent the transfer coefficient, respectively, for reactions (1) or (2).  $E_M$  is the electrode potential of the sensing electrode at the equilibrium state, so it is called a mixed potential. The constants  $A$ ,  $n$  and  $m$  changed with the operating temperature [14], so that the EMF value of the sensor decreased along with the increased operating temperature at the same concentration in Fig. 6. When the concentration of oxygen is fixed, the mixed potential changes linearly with the logarithm of the concentration of  $NH_3$ , as described in Eq. (5)

$$E_M = E'_0 - mA \ln C_{NH_3} \quad (5)$$

Here,  $E'_0 = E_0 + nA \ln C_{O_2}$

Eq. (5) could explain the experimental results very well. Similar reactions above occur at the contacting electrode possibly. But the EMF is smaller than that of the sensing electrode. So the electrochemical reactions occurring at the sensing electrode are dominant to that of the contacting electrode.

#### 4. Conclusions

A compact solid electrolyte sensor using a thick film of NASICON and porous  $Cr_2O_3$  electrode has been examined to show good sensing properties to dilute ammonia. The slope between the EMF and the logarithm of ammonia concentration was  $-89$  mV/decade, and the 90% response time to 50 and 500 ppm ammonia was 35 and 30 s, respectively, and the recovery time was 60 and 65 s, respectively. In addition, the sensor also showed excellent selectivity to ammonia against the disturbing gases, and the operating temperature of the sensor was  $350^\circ C$ . Mixed potential theory could explain the sensing behavior of the sensor. However, further study on the sensing mechanism is yet to be done for understanding the electrochemical behavior at the sensing electrode very well.

#### Acknowledgements

The financial support of Natural Science Foundation of China (No. 60574096) and National Science Fund for Distinguished Young Scholars of China (No. 60625301) is gratefully acknowledged.

#### References

- [1] D. Patil, L. Patil, P. Patil,  $Cr_2O_3$ -activated ZnO thick film resistors for ammonia gas sensing operable at room temperature, *Sens. Actuators B: Chem.* 126 (2007) 368–374.
- [2] A. Satsuma, K. Shimizu, K. Kashiwagi, T. Endo, H. Nishiyama, S. Kakimoto, S. Sugaya, H. Yokoi, Ammonia sensing mechanism of tungstated-zirconia thick film sensor, *J. Phys. Chem. C* 111 (2007) 12080–12085.
- [3] T. Fua, J. Tao, Novel highly-selective  $NH_3$  sensor based on potassium trisoxalate-ferrate(III) complex, *Sens. Actuators B: Chem.* 129 (2008) 339–344.
- [4] P. Lauque, M. Bendahan, J. Seguin, K. Ngo, P. Knauth, Highly sensitive and selective room temperature  $NH_3$  gas microsensor using an ionic conductor (CuBr) film, *Anal. Chim. Acta* 515 (2004) 279–284.
- [5] S. Dhawana, D. Kumar, M. Ram, S. Chandra, D. Trivedi, Application of conducting polyaniline as sensor material for ammonia, *Sens. Actuators B: Chem.* 40 (1997) 99–103.
- [6] M. Matsuguchi, J. Ito, G. Sugiyama, Y. Sakai, Effect of  $NH_3$  gas on the electrical conductivity of polyaniline blend films, *Syn. Met.* 128 (2002) 15–19.
- [7] S. Tao, L. Xu, J. Fanguy, Optical fiber ammonia sensing probes using reagent immobilized porous silica coating as transducers, *Sens. Actuators B: Chem.* 115 (2006) 158–163.
- [8] F. Qiu, Q. Zhu, X. Yang, Y. Quan, B. Xu, Preparation of planar  $CO_2$  sensor based on solid-electrolyte NASICON synthesized by sol-gel process, *Mater. Chem. Phys.* 83 (2004) 193–198.
- [9] X. Liang, Y. He, F. Liu, et al., Solid-state potentiometric  $H_2S$  sensor combining NASICON with  $Pr_6O_{11}$ -doped  $SnO_2$  electrode, *Sens. Actuators B: Chem.* 125 (2007) 544–549.
- [10] B. Min, S. Choi,  $SO_2$ -sensing characteristics of Nasicon sensors with  $Na_2SO_4$ - $BaSO_4$  auxiliary electrolytes, *Sens. Actuators B: Chem.* 93 (2003) 209–213.
- [11] G. Lu, N. Miura, N. Yamazoe, High-temperature sensors for NO and  $NO_2$  based on stabilized zirconia and spinel-type oxide electrodes, *J. Mater. Chem.* 7 (1997) 1445–1449.
- [12] G. Lu, N. Miura, N. Yamazoe, High-temperature hydrogen sensor based on stabilized zirconia and a metal oxide electrode, *Sens. Actuators B: Chem.* 35–36 (1996) 130–135.
- [13] Y. Shimizu, H. Nishi, H. Suzuki, K. Maeda, Solid-state  $NO_x$  sensor combined with NASICON and Pb-Ru-based pyrochlore-type oxide electrode, *Sens. Actuators B: Chem.* 65 (2000) 141–143.
- [14] X. Liang, T. Zhong, B. Quan, et al., Solid-state potentiometric  $SO_2$  sensor combining NASICON with  $V_2O_5$ -doped  $TiO_2$  electrode, *Sens. Actuators B: Chem.* 134 (2008) 25–30.

#### Biographies

**Xishuang Liang** received the B Eng degree in department of electronic science and technology in 2004. He is currently studying for his Dr Sci degree in College of Electronic Science and Engineering, Jilin University, China. His current research is solid electrolyte gas sensor.

**Tiegang Zhong** received the B Eng degree in department of electronic sciences and technology in 2005. He is currently studying for his MSc degree in College of Electronic Science and Engineering, Jilin University, China. He is currently studying for his Dr Sci degree in College of Electronic Science and Engineering, Jilin University, China. His current research is chemical gas sensor.

**Hesong Guan** received the B Eng degree in department of electronic science and technology in 2004. He is currently studying for his Dr Sci degree in College of Electronic Science and Engineering, Jilin University, China. His current research is surface analysis.

**Fengmin Liu** received her Doctor's degree in College of Electronic Science and Engineering at Jilin University in 2005. Her current research interests are the application of nanomaterials and microdevices.

**Geyu Lu** received the B Sci degree in electronic sciences in 1985 and the M Sci degree in 1988 from Jilin University in China and the Dr Eng degree in 1998 from Kyushu University in Japan. Now he is a professor of Jilin University, China.

**Baofu Quan** graduated from Jilin University in 1969. He is a professor of Jilin University, China. His current research is on the characteristics and development of oxide semiconductors (gas sensors material) and solid electrolyte gas sensor.